Contrast of Surface Heating Between *El Nino* and *La Nina*

Ming-Dah Chou, Shu-Hsien Chou, Shuk-Mei Tse
Department of Atmospheric Sciences,
National Taiwan University

Abstract

The heating of the tropical Pacific and its relation with the sea surface temperature (SST) is investigated for the period 1987-1995 using the radiative and turbulent fluxes derived from satellite observations and reanalyses. The data show that during an *El Nino* year when the central and eastern equatorial Pacific is abnormally warm, the surface solar radiation reduces due to enhanced cloudiness, and the surface evaporation increases due primarily to increases in the air-sea humidity difference. The combined effect is to reduce the heating of the ocean during a warm *El Nino* episode. On the other hand, during a *La Nina* year, when the central and eastern equatorial Pacific is anomalously cool, the reverse is true; an enhance solar heating due to reduced cloudiness, and an reduced surface evaporation due to reduced air-sea humidity difference, leading to a net heating of the equatorial Pacific. Thus, the surface heating has a stabilizing effect on SST; the surface heating is anomalously low during a warm episode and anomalously high during a cool episode. Even though the surface heating is highly correlated with SST during *El Nino* and *La Nina*, the correlation is very weak during normal years. As a result, the surface heating is only weakly correlated with SST over an extended period of time. Because the surface heating can only reduce the intensity of *El Nino* and *La Nina*, the mechanisms that trigger *El Nino* and *La Nina* must be the dynamics of ocean mixed layer, such as the delayed action oscillator or the overshooting of heat divergence as previously proposed by investigators.

Key word: Sea surface temperature, surface heat budgets, El Nino, La Nina.

1. Introduction

Taiwan borders the massive Asian continent and the Pacific Ocean, and its climate is very sensitive to the thermal heating of the Asian continent and the location and strength of the North Pacific high pressure system. The Asian and North Pacific pressure systems affect the seasonal East Asian monsoons as well as the interannual El Nino/Southern Oscillations (ENSO), which in turn significantly affect the climate of Taiwan. There are different views on the origin of the ENSO. The delayed action oscillation theory (Suarez and Schopf, 1988) involves the oceanic wave transit effects through a negative, delayed feedback. Whereas the heat pump theory (Sun, 2000) involves heating of the ocean during the cold phase of the ENSO (El Nina) and cooling of the ocean during the warm phase of the ENSO (El Nino). During a La Nina, the central and eastern tropical Pacific is cool and dry. Evaporative cooling is weak and solar heating is strong. During an El Nino, on the other hand, the central and eastern tropical Pacific is warm and cloudy. Evaporative cooling is strong and solar heating is weak. Thus the surface heating acts as a modulator for the sea surface temperature (SST), and information on both the radiative and turbulent fluxes at the sea surface is essential for studying the climate oscillation in the tropical Pacific.

To understand the intraseasonal and interannual variations of SST, the information on the seasonal to variability of the surface heat budget and the correlation of surface heating with SST tendency in the tropical warm pool is particularly important. Chou et al. (2004) investigated the seasonal to interannual variations of the To understand the intraseasonal and interannual variations of SST, the information on the seasonal to variability of the surface heat budget and the correlation of surface heating with SST tendency in the tropical warm pool is particularly important. Chou et al. (2004) investigated the seasonal to interannual variations of the surface heat budgets and their relationships to SST tendency over the tropical eastern Indian and western Pacific Oceans (30°S–30°N, 90°E–170°W) during a 3-yr period of October 1997–September 2000. This period included the strong 1997/98 El Nino warm event, and the moderate 1998/99 La Nina cold event. They found that the correlation between interannual variations of surface heating and SST tendency is weak, indicating the importance of ocean dynamics in affecting the interannual SST variations.

As limited by the domain and period of the GMS-retrieved surface radiation data, the work of Chou et al. (2004) only covered the tropical eastern Indian Ocean and western Pacific for three year. In this study, we extend the work of Chou et al. to investigate the relation between surface heating and SST by including five different sea surface heat flux data and covering the entire tropical Pacific for a period of 8 years.

2. Datasets

The data used for heat budget analysis are 1° latitude-longitude monthly mean surface radiative and turbulent heat fluxes, sea surface temperature, surface wind speed (U_{10m}), and sea-air humidity difference (q^*-q_a) during the 8-yr period of 1988-1995. Data are either from observation or from reanalysis. Data are either from observations or from reanalysis. The observation-based data include radiative fluxes from NASA/GEWEX SRB_Rel2 (Stackhouse et al. 2002; Gupta et al. 2004) and the turbulent fluxes from the GSSTF2 (Chou et al. 2003) and HOAPS-II (Grassl et al. 2000). The reanalysis include the NCEP/NCAR reanalysis data (Kalnay et al. 1996) and the ECMWF ERA-40 reanalysis. The SST are taken from the NCEP/NCAR analysis (Reynold and Smith, 1994).

3. Mean fluxes

The net surface heat flux, F_{NET}, comprises four components, solar radiation (or shortwave, SW), infrared (or longwave, LW), latent heat, and sensible heat fluxes. It given by

$$F_{NET} = F_{SW} - F_{LW} - F_{LH} - F_{SH}$$

where the subscripts *SW*, *LW*, *LH*, and *SH* denote shortwave, longwave, latent heat, and sensible heat, respectively. For F_{NET} and F_{SW}, downward flux is positive. Whereas for F_{LW}, F_{LH}, and F_{SH}, upward flux is positive. Because F_{LW} and F_{SH} are small, we show only the results for F_{SW}, F_{LH}, and F_{NET}.

The surface solar, latent heat, and net heat fluxes averaged over the tropical Pacific and the seven-year period from Jan 1988 to Dec 1994 are shown in Figure 1. The net surface flux is computed from Eq. (1) with radiative fluxes taken from the SRB_Rel2 data archive and the turbulent fluxes from the GSSTF2 data archive. It can be seen that the maximum solar heating and evaporative cooling is in the subtropical high pressure regions where the atmosphere is dry and clear, the trade winds are strong, and the air-sea humidity difference is large. The region of minimum evaporative cooling is near the equator where the winds are converging and weak. On the other hand, the region of the minimum solar heating is just north of the equator where the mean ITCZ is located. The bottom panel of the figure shows that the maximum net surface heating is located at the equator where solar heating is strong and evaporative cooling is weak. Whereas the minimum net surface heating is located at the subtropical high pressure regions where the strong solar heating and evaporative cooling offset each other. The magnitude of solar heating is significantly (~270 Wm^{-2}) larger than that of the evaporative cooling (~180 Wm^{-2}), but the spatial variation of the former (~70 Wm^{-2}) is smaller than that of the latter (~130 Wm^{-2}). As a result, the spatial variation of the net surface heating is predominantly determined by the evaporative cooling (Chou et al., 2004).

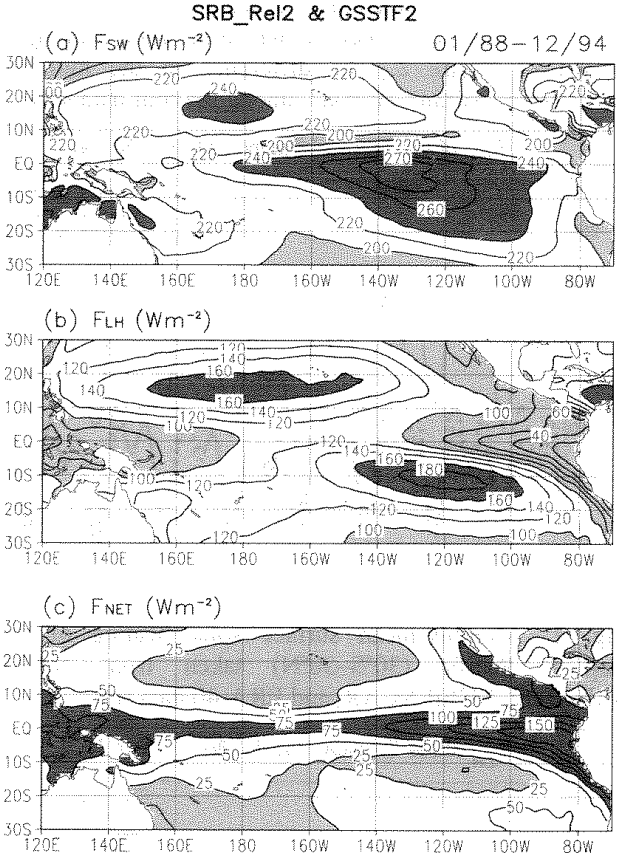

Fig. 1. Surface solar heating, evaporative cooling, and net heating, averaged over the 7-yr period Jan 1988–Dec 1994. In computing the net heating, turbulent fluxes are taken from GSSTF2 and radiative fluxes are taken from NASA SRB_Rel2.

The monthly mean surface solar heating averaged over the tropical Pacific for the SRB_Rel2, NCEP/NCAR, and ERA–40 are shown in Figure 2. The solar heating from reanalyses is systematically smaller than the satellite retrieval by 20–25 Wm^{-2}. The underestimation of solar heating in the reanalyses is likely due to overestimation of low level clouds in GCM model simulations. Nevertheless, the time variations of the analyses follow closely that of the satellite retrieval. As judged from the surface solar heating, the cloudiness in the Pacific has a maximum in June when the sun is at the extreme north location and a secondary weak maximum in December when the sun is at the extreme south location. At equinox when the sun crosses the equator, the solar heating is a maximum and the cloudiness is a minimum.

Compared to the surface solar heating, the evaporative cooling, shown in Figure 3, is significantly close to each other among the four data sets, especially after Jan 1993. It is interesting that the evaporative cooling of the GSSTF2 has a positive trend during the 7-yr period. It is likely due to increases in either SST or winds. This positive trend in evaporation implies a strengthened atmospheric hydrological cycle which might be related to global warming. Figure 4 shows the

variations of the monthly mean net surface heating. The large difference between those based on observations and those of reanalyses reflect the bias in the solar heating as shown in Figure 2. The difference in the monthly variations is within ~10 Wm^{-2} among the four data sets.

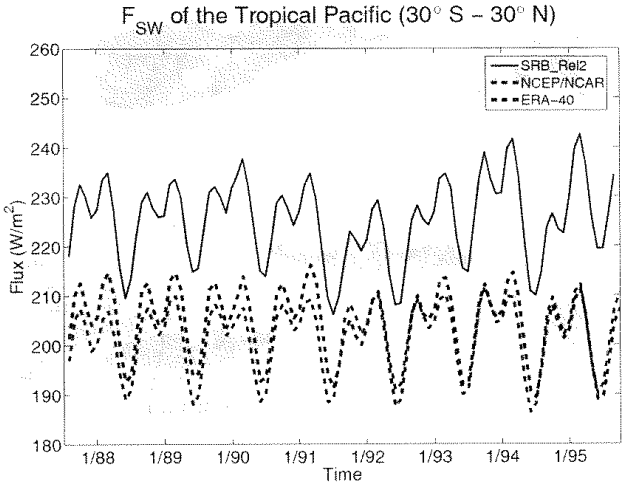

Fig. 2. Monthly-mean surface solar heating of the tropical Pacific (30°S–30°N) taken from NASA SRB_Rel2, NCEP/NCAR, and ERA-40 data sets.

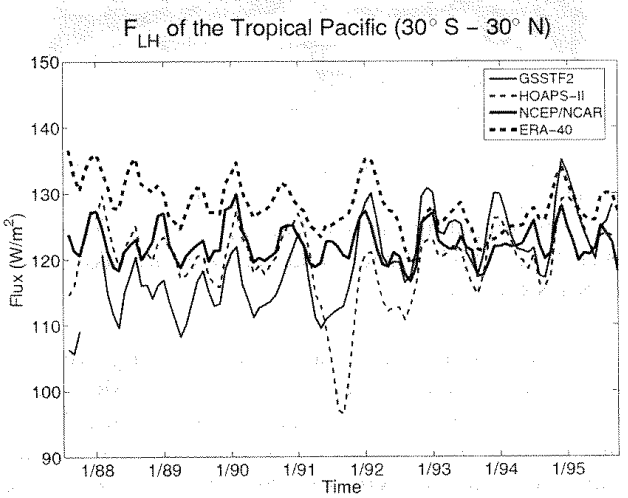

Fig. 3. Monthly-mean evaporative cooling of the tropical Pacific (30°S–30°N) taken from GSSTF2, HOAPS-II, NCEP/NCAR, and ERA-40 data sets.

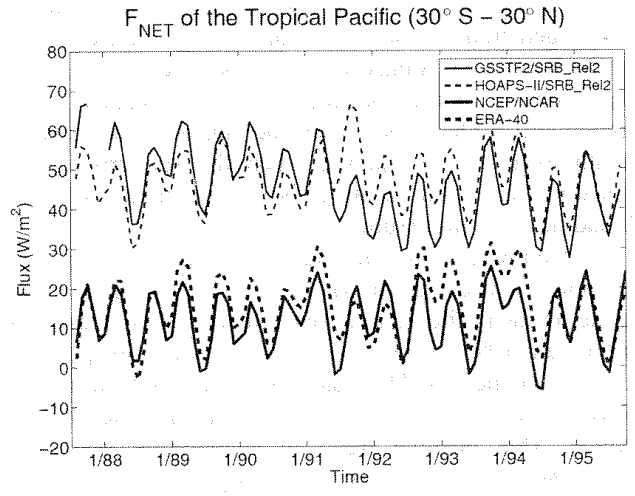

Fig. 4. Same as Fig. 3, except for the net heating.

4. 1991/1992 El Nino and 1988/89 La Nina

During the 7-yr period from 1988 to 1994, there is an El Nino which peaks in the winter of 1991/92 and a La Nina which peaks in the winter of 1988/89. The SST in the Nino 3.4 (5°S–5°N, 170°W–120°W) is anomaly higher by 2°C in the former episode and lower by the same magnitude in the latter episode. During these two episodes, the clouds, atmospheric and oceanic circulation, and the heat exchanges at the air–sea interface also undergo significant changes. Figure 5 shows changes between the El Nino and the La Nina in the surface heat fluxes, SST, the 10–m height wind speed, and the air–sea humidity difference at the 10–m height (denoted as ΔF, ΔT_s, ΔU, and $\Delta\ (q^*\text{-}q_a)$, respectively). Those quantities are mean values of the winter 6-months (October–March) of each episode. Except for the radiative fluxes, all other parameters are taken from the GSSFT2 data archive. The solar and IR radiative fluxes are taken from SRB_Rel2.

During the El Nino the tropical central and eastern Pacific is much warmer than the La Nino by 4°C (Fig. 5a). Correspondingly, the deep convective and high cloudiness center shifted eastward from the warm pool to the central equatorial Pacific. The solar heating (Fig. 5d) is much reduced, with ΔF_{SW} reaching-75 Wm^{-2}, over most of the tropical Pacific, except in the warm pool and the South Pacific Convergence Zone (SPCZ). The surface winds are weakened during the El Nino in the trade wind regions but enhanced in the equatorial eastern Pacific (Fig. 5b), whereas $\Delta\ (q^*\text{-}q_a)$ increases nearly across the entire tropical Pacific (Fig. 5c) primarily due to the increase of the saturation surface humidity associated with temperature increase. The change of evaporative cooling in the El Nino is largely positive (Fig. 5e). The ΔF_{LH} in the equatorial eastern Pacific reaches 75 Wm^{-2}, which is a result of large increases of ΔU and $\Delta\ (q^*\text{-}q_a)$. The weakened trade winds during the El Nino cause a weakened evaporative cooling in the equatorial central Pacific during the El Nino. The change of the net surface flux is shown in Fig. 5f. Except for some scattered regions, the tropical Pacific experiences a reduced heating at the surface during the El Nino, as was also noticed by Sun (2000). The maximum reduction of surface net heating, –75 Wm^{-2}, is located in the equatorial eastern Pacific, which is a result of a moderate reduction of solar heating combined with a large increase of evaporative cooling.

The longitudinal distributions of the changes of F_{SW}, F_{LH}, and F_{NET}, in the equatorial Pacific (10°S–10°N) between the El Nino and La Nina are shown in Fig. 6 for the various data sets. For the GSSTF2/SRB_Rel2 and HOAPS-II/SRB_Rel2, the turbulent fluxes are taken from GSSTF2 and HOAPS-II and the radiative fluxes are taken from SRB_Rel2. For the change of solar heating (upper panel), SRB_Rel2 and ERA–40 follow closely each other, regardless of the large bias of the 7–yr means as shown in Fig. 2. It indicates that the cloud amount of the ERA_40 reanalysis is too high, but the longitudinal variation of clouds is reasonable. The solar heating enhances during the El Nino by ~40 Wm^{-2} in the warm

pool and reduces by 60 Wm^{-2} in the central equatorial Pacific. For the NCEP/NCAR, the longitudinal variation of ΔF_{SW} is much smaller than the other two data sets. As judged from Fig. 2 and the outgoing longwave radiation (not shown), the amount of low–level cloud of the NCEP/NCAR is too high, so there is not much room for the change in cloud amount between El Nino and La Nina.

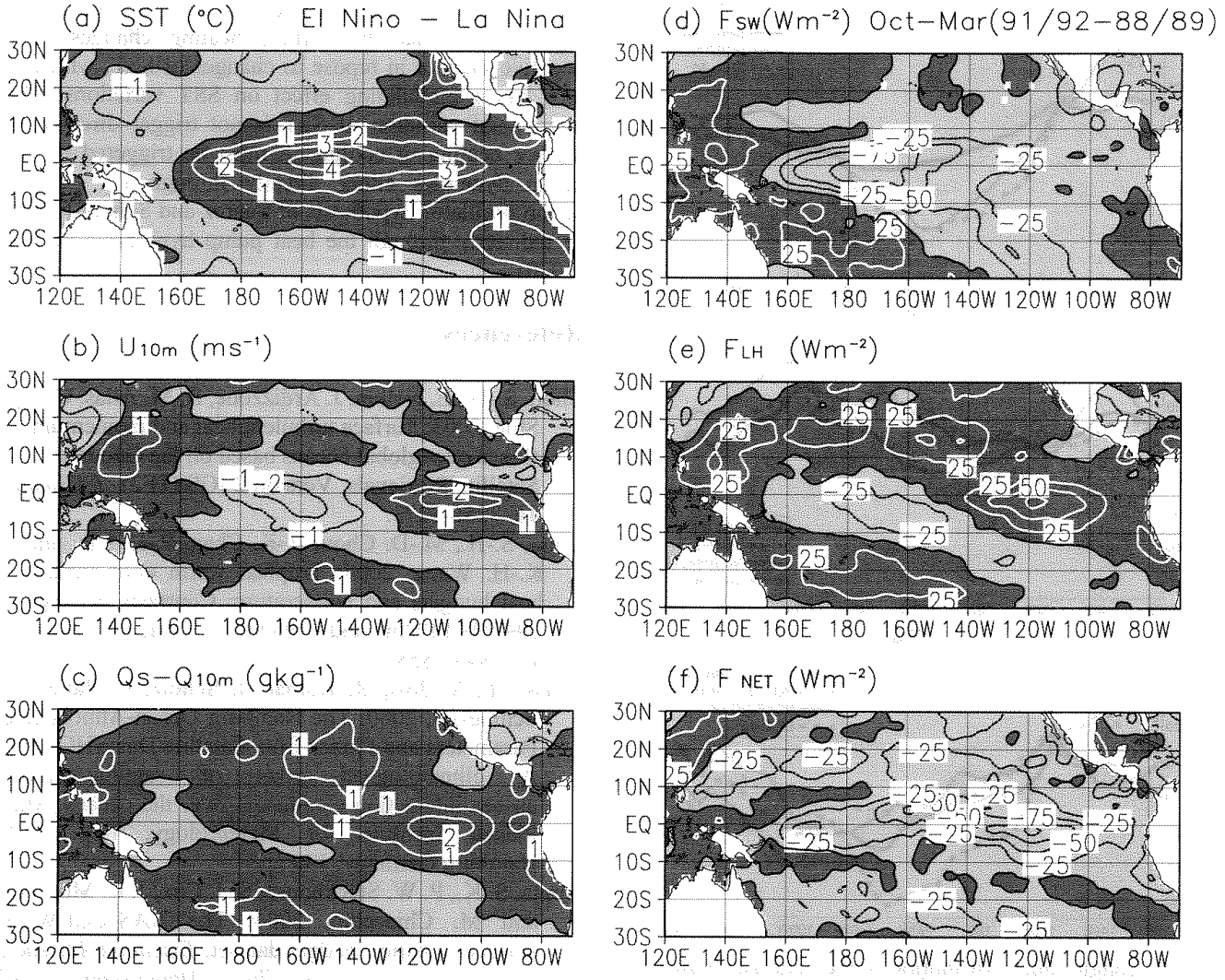

Fig. 5. Contrasts between the 91/92 El Nino and the 88/89 La Nina of the SST, wind, air-sea humidity difference surface solar heating, evaporative cooling, and net heating,. Data are taken from GSSTF2, except for the solar heating which is taken from the NASA SRB_Rel2 data archive.

The longitudinal distributions of ΔF_{LH} are shown in the middle panel of Fig. 6. The discrepancy in ΔF_{LH} among the four data sets is comparable to that of ΔF_{SW}. In the Pacific warm pool, the ΔF_{LH} ranges from +30 Wm^{-2} for GSSTF2 to -20 Wm^{-2} for HOAPS-II. Relative to GSSTF2, HOAPS-II has smaller ΔU and $\Delta(q^*-q_a)$, which is the cause for a small ΔF_{LH} for HOAPS-II in the warm pool. The ΔF_{LH} of NCEP/NCAR and ERA–40 follow each other closely across the equatorial Pacific.

The longitudinal distributions of ΔF_{NET} are shown in the lower panel of Fig. 6. The ocean losses heat in the equatorial Pacific except the warm pool west of 160°E. During the El Nino, convection center shifted to the central Pacific, and the ΔF_{SW} is positive in the warm pool region (upper panel). Except for the HOAPS-II, both ΔU and ΔF_{LH} are positive, leading to a small ΔF_{NET} in the warm pool. For the HOAPS-II/SRB_Rel2, the ΔU and ΔF_{LH} are negative, which in combination with a large positive ΔF_{SW} leads to a large positive ΔF_{NET}. The reduced surface heating in the central equatorial Pacific during the El Nino is very large for the HOAPS-II/SRB_Rel2, reaching 80 Wm^{-2} at 150°W.

5. Sea Surface heating and SST

In the search for the origin of the tropical intraseasonal and interannual oscillations, it is important to understand the correlation between the surface heating and SST as to what degree the surface heating affects the SST and, conversely, the surface heating responses to SST. In Fig. 7 we show the time series of monthly F_{NET} and SST anomalies over the Nino 3.4 region for the period July 1987 August 1995. It appears that the F_{NET} anomaly and the negative SST anomaly follow each other rather well for all the four data sets. At the extreme sea surface temperature in Jan 1989, Jan 1992, and Dec

1994, the F_{NET} anomaly are ~30, –40, and –25 Wm^{-2} for all the four data sets, except for the NCEP/NCAR in Jan 1992 when the F_{NET} anomaly is –80 Wm^{-2}.

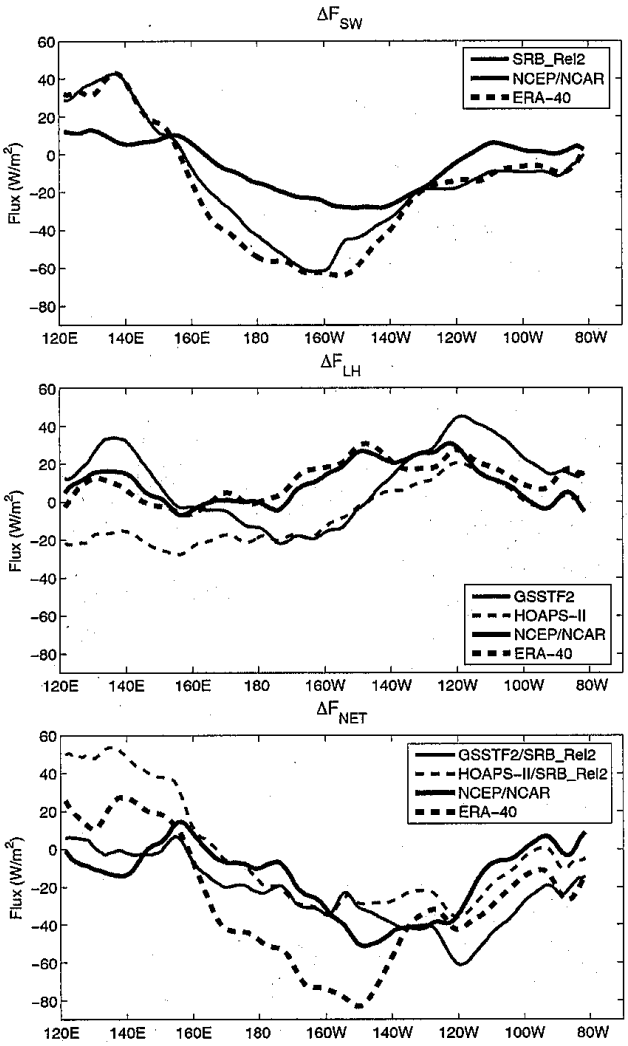

Fig. 6. Longitudinal distribution of the contrasts between the 91/92 El Nino and the 88/89 La Nina of the surface net heating in the latitude band 10°S–10°N. For the GSSTF2 and HOAPS-II, the NASA SRB_Rel2 radiative fluxes are used in computing the surface net heating.

The lag correlation between SST and the surface heat fluxes are shown in Fig. 8 for the four data sets. For all the data sets, there does not seem to have any significant lags. The correlation coefficient is a maximum at zero–lag and nearly symmetric relative to the zero–lag. The correlation is significantly higher for the reanalyses than the correlation for the observation–based data sets. In the reanalyses, the SST is given as an input data for model simulation, and the surface heat fluxes are the response to the specified SST field. It is reasonable to expect a high correlation between SST and the surface heating. On the other hand, the observation–based surface heat fluxes are derived from many parameters, and the SST is only one of the parameters. The correlation between SST and the surface heating is not necessary high. This is especially true for the GSSTF2/SRB_Rel2, where there is no correlation between SST and F_{LH}, and the maximum correlation between SST and F_{NET} at zero–lag is only 0.38. The weak and zero–lag nature of the correlation implies the importance of large scale-circulation in affecting the surface heating. The negative and zero–lag correlation also implies that the surface heating changes in a negative manner in repose to changes of SST, which in turn has a modulating effect on SST variations. The interannual variation of SST is not trigger directly by surface heating or cooling. It must be triggered by the ocean dynamics either directly through the delayed action oscillator hypothesis of Suarez and Schopf (1988) or indirectly through the heat pump hypothesis of Sun (2000).

References

Chou, S.-H., E. Nelkin, J. Ardizzone, R. M. Atlas, C.-L. Shie, 2003: Surface turbulent heat and momentum fluxes over global oceans based on the Goddard Satellite Retrievals, Version 2 (GSSTF2), *J. Climate,* **16**, 3256-3273.

Chou, S.-H., M.-D. Chou, P.-K. Chan, P.-H. Lin, and K.-H. Wang, 2004: Tropical warm pool surface heat budgets and temperature: Contrasts between 1997/98 El Nino and 1998/99 La Nina, *J. Climate,* **17**, 1845-1858.

Grassl H., V. Jost, R. Kumar, J. Schulz, P. Bauer, P. Schluessel, 2000: The Hamburg Ocean-Atmosphere Parameters and Fluxes from Satellite Data (HOAPS): A climatological atlas of satellite-derived air-sea-interaction parameters over the oceans. Max Planck Institute for Meteorology, Rep. 312, Hamburg Germany, 130 pp.

Gupta, S. K., P. W. Stackhouse, S. J. Cox, J. C. Mikovitz, and M. Chiacchio, 2004: The NASA/GEWEX surface radiation budget dataset. *Extended Abstract, 13th Conf. on Satellite Meteorology and Oceanography*, Norfolk, VA, Amer. Meteor. Soc., CD-ROM, P6.6.

Kalnay, E., and coauthors, 1996: The NCEP/NCAR 40-year reanalysis project. *Bull. Amer. Meteorol. Soc.*, **77**, 437-471

Reynolds, R. W. and T. M. Smith, 1994: Improved global sea surface temperature analyses, *J. Climate,* **7**, 929-948.

Stackhouse, P. W., S. K. Gupta, S. J. Cox, J. C. Mikovitz, and M. Chiacchio, 2002: New results from the NASA/GEWEX surface radiation budget project: Evaluating El Nino effects at different scales. *Extended Abstract, 11th Conf. on Atmospheric Radiation*, Ogden, UT, Amer. Meteor. Soc., CD-ROM, P3.6.

Suarez, M., J., and P. Schopf, 1988: A delayed action Oscillator for ENSO. *J. Atmos. Sci.*, **45**, 3283–3287.

Sun, D. –Z., 2000: The heat sources and sinks of the 1986–1987 El Nino. *J. Climate*, **13**, 3533-3550.

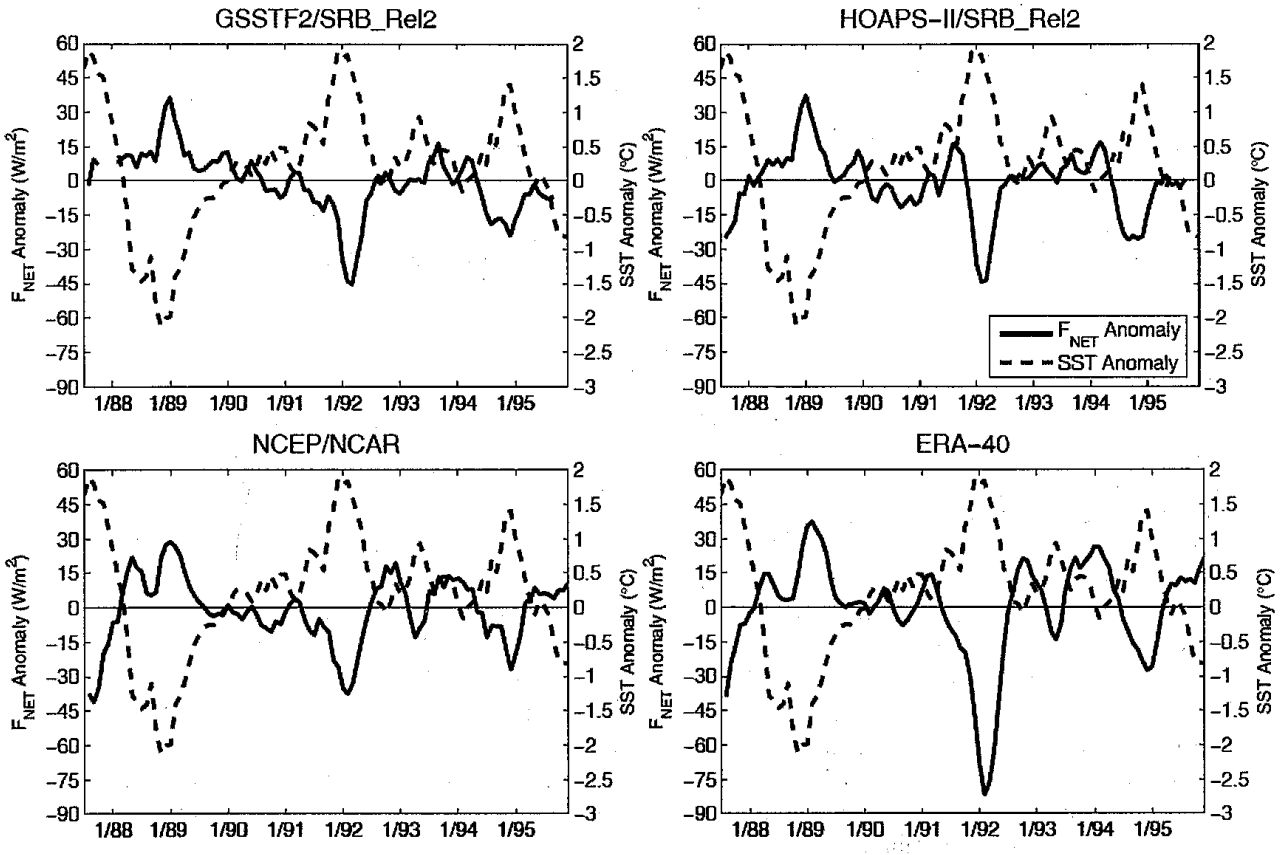

Fig. 7. Monthly anomaly of SST of the Nino-3.4 and surface net heating of the region 5°S–5°N; 120°W–170°W. For the GSSTF2 and HOAPS-II, the SRB_Rel2 radiative fluxes are used in computing the surface net heating.

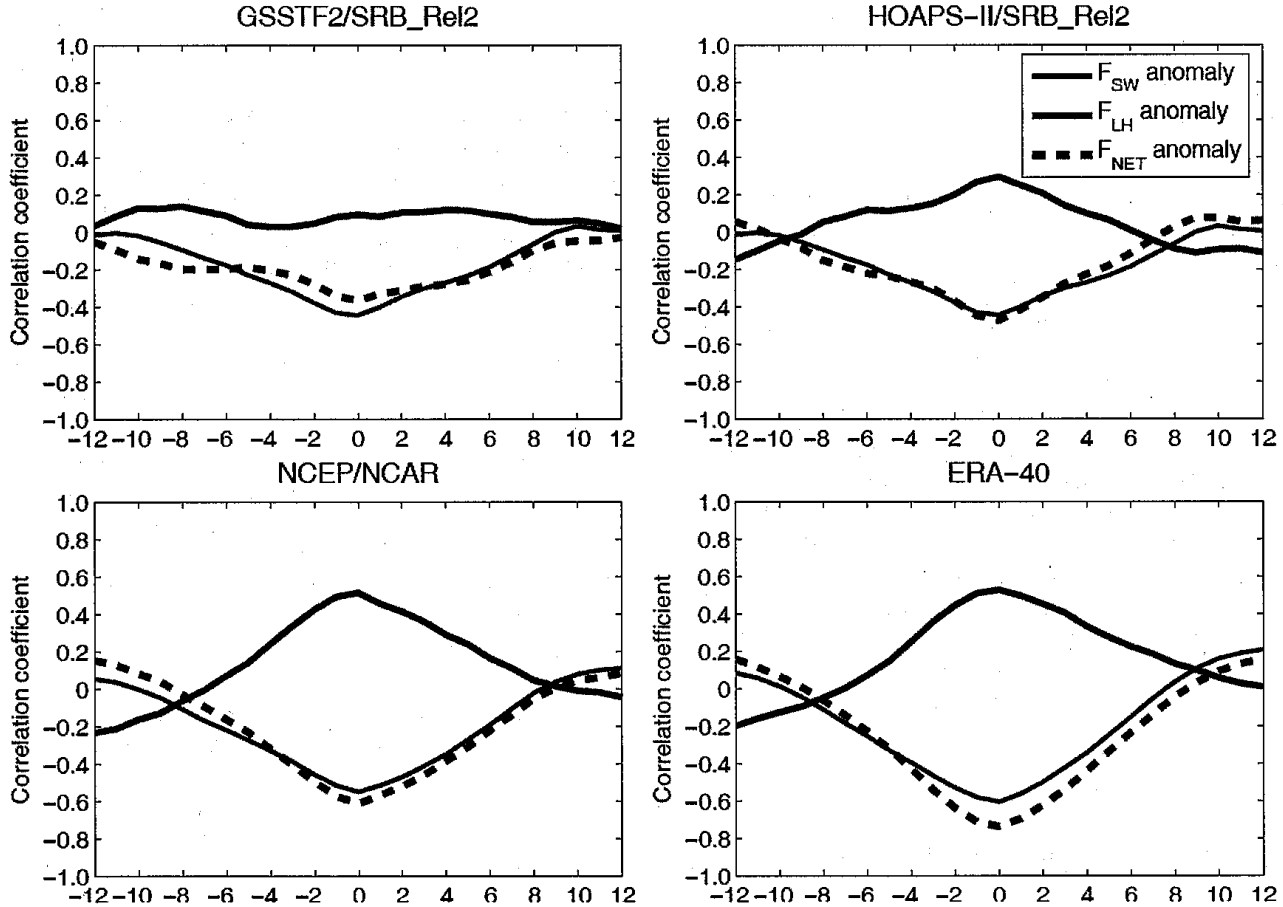

Fig. 8. Correlation coefficient of between the SST and the surface solar, latent heat, and net heat fluxes. Positive number of months indicates SST leading heat fluxes.